THE JOURNAL OF BIOLOGICAL CHEMISTRY
Vol. 272, No. 40, Issue of October 3, pp. 25339–25344, 1997
Printed in U.S.A.

Vacuoles Induced by *Helicobacter pylori* Toxin Contain Both Late Endosomal and Lysosomal Markers*

(Received for publication, April 29, 1997, and in revised form, July 21, 1997)

Maurizio Molinari‡§, Carmela Galli‡, Nathalie Norais¶, John L. Telford¶, Rino Rappuoli¶, J. Paul Luzio‖, and Cesare Montecucco‡

From the ‡Centro CNR Biomembrane and Dipartimento di Scienze Biomediche, Università di Padova, 35100 Padova, ¶Centro Ricerche IRIS, Biocine-Chiron, 53100 Siena, Italy, and the ‖Department of Clinical Biochemistry, University of Cambridge, Cambridge CB2 2QR, United Kingdom

Intoxication of mammalian cells with the vacuolating toxin (VacA) released by *Helicobacter pylori* causes the formation of large acidic vacuoles containing the vacuolar ATPase proton pump and Rab7, a late endosome marker. Here, we describe a novel subcellular fractionation procedure, and we show that nanomolar concentrations of VacA induce a clear redistribution of lysosomal membrane glycoproteins among endocytic compartments. This redistribution is an early event in the process of cellular intoxication by VacA and precedes the formation of macroscopic vacuoles. The absence of the cation independent mannose 6-P receptor and the presence of Rab7 and of lysosomal membrane proteins in the newly formed compartment suggest that the vacuolating toxin induces the accumulation of a post-endosomal hybrid compartment presenting both late endosomal and lysosomal features.

Helicobacter pylori, a Gram-negative, spiral-shaped bacterium colonizing the stomach, is involved in the pathogenesis of gastritis and gastroduodenal ulcers (1, 2). Recently, such an infection has been associated to MALT lymphomas and to an increased risk of developing gastric adenocarcinoma (3–6). Even though *H. pylori* shows a great genetic variability, strains isolated from human biopsies can be classified into two groups (7). Type I strains are associated with the more serious pathologies and are characterized by the common production of a toxin, termed VacA,[1] and of a toxin-associated antigen (CagA). Type II strains produce neither of these two antigens and lack a 40-kilobase pathogenicity island found in the genome of type I strains (8). VacA is synthesized as a 140-kDa precursor, which is processed to the mature 95-kDa protein during export from the bacteria (9–11). Structural features of the toxin (9, 12) hint at the possibility that VacA belongs to the group of bacterial protein toxins with an A-B type structural organization: protomer B binds to a membrane receptor present on the surface of target cells and mediates the translocation of the catalytic A subunit into the cell cytosol (13).

Intoxication of cells with VacA perturbs the endocytic traffic at a late stage, and large acidic vacuoles with elements of late endosomal compartments are formed (14–17). The analysis of the early events of cellular intoxication and an accurate mapping of the main vacuolar components will help in determining the intracellular target(s) of VacA and in understanding the mechanism of cellular intoxication by this novel bacterial toxin.

Baby hamster kidney (BHK) is a cell line often used in studies of the endocytic path of higher eucaryotes. The route leading endocytosed material from the plasma membrane of BHK cells, through the early endosomal compartment ($Rab5^+$/transferrin receptor$^+$) to the late endosomal compartment ($Rab7^+$/cation independent mannose 6-P receptor (CI-M6PR)$^+$), has been characterized in detail using electron microscope markers and a range of Rab mutants and/or endocytosis inhibitors (18–22). However, the distal part of the endocytic path, connecting late endosomal compartments to lysosomes, is less characterized (22, 23).

Here, BHK cells exposed to VacA were fractionated with a novel, isopycnic density ultracentrifugation method, optimized for the purification of late endosomes and lysosomes from BHK cells. Together with parallel immunofluorescence staining, this procedure allowed us to obtain evidence that vacuoles are enriched in lysosomal membrane markers such as Lgp110, contain low levels of lysosomal hydrolytic activities, are characterized by the presence of the late endocytic marker Rab7, but are devoid of another late endosomal marker, the CI-M6PR. These results indicate that VacA induces the formation and pathological accumulation of a mixed endo-lysosomal compartment.

EXPERIMENTAL PROCEDURES

Reagents—Rabbit polyclonal anti-rat CI-M6PR was a kind gift of Dr. B. Hoflack (Institut Pasteur de Lille, France); rabbit polyclonal anti-VacA was produced and characterized as described previously (24); rabbit polyclonal anti-rat Lgp110 was as described in Reaves *et al.* (29). Rabbit polyclonal antibody to Rab7 was a kind gift of Dr. M. Zerial (EMBL, Heidelberg, Germany). Rabbit anti-human cathepsin D and cathepsin B were purchased from Calbiochem, Texas Red-labeled donkey anti-rabbit was from Amersham Corp. (Little Chalfont, UK). β-Glucosaminidase and acid phosphatase activities were determined using *p*-nitrophenyl-*N*-acetyl-β-D-glucosaminide and *p*-nitrophenyl phosphate disodium (Sigma) as substrates. Optiprep™ was purchased from Life Technologies, Inc. (Milan, Italy).

Cell Culture and Intoxication—Baby hamster kidney (BHK) cells were grown in Dulbecco's modified Eagle's medium, 10% fetal calf serum in an incubator with 5% CO_2, at 37 °C. Twelve to 24 h before the beginning of the experiments, cells were seeded in Petri dishes with a density of 65–130,000 BHK/cm^2. Highly purified VacA was prepared and activated by short acid exposure as described (24, 25), neutralized by addition of Dulbecco's modified Eagle's medium, 2% fetal calf serum (intoxication medium), and added to BHK cells. Incubation time was 4 h for all the experiments, the concentration of VacA used is specified in the description of every experiment. Cell vacuolation as presented in

* This work was supported by Ministero Pubblico Instruzione (40%) and by Human Capital Mobility Grant CHRX CT 920018 (60%). The costs of publication of this article were defrayed in part by the payment of page charges. This article must therefore be hereby marked "*advertisement*" in accordance with 18 U.S.C. Section 1734 solely to indicate this fact.

§ Supported by a long term EMBO fellowship. To whom correspondence should be addressed: Centro CNR Biomembrane and Dept. di Scienze Biomediche, Università di Padova, Via G. Colombo 3, 35100 Padova, Italy. Fax: 0039-49-8276049; E-mail: toxin@civ.bio.unipd.it.

[1] The abbreviations used are: VacA, vacuolating toxin; BHK, baby hamster kidney; CI-M6PR, cation independent mannose 6-P receptor; LE, late endosome(s); Lgp, lysosomal membrane glycoprotein(s); PNS, post-nuclear supernatant; PBS, phosphate-buffered saline; PAGE, polyacrylamide gel electrophoresis.

Fig. 4 was quantified by determining the total neutral red uptake (26).

Fractionation of Organelles by Sucrose Step Gradient—Fractionation of organelles of BHK cells (treated with 5 nM VacA and mock-treated) by sucrose step gradient was performed essentially as described (27), in a cold room. Briefly, cells were carefully washed with ice-cold isotonic phosphate buffer, pH 7.4 (PBS), scraped with a rubber policeman, and pelleted by centrifugation in a table centrifuge (750 rpm, 5 min). They were then resuspended in 3 ml of homogenization buffer (HB-EDTA, 3 mM imidazole, pH 7.4, 250 mM sucrose (8%), 1 mM EDTA, 1 μg/ml antipain, 10 μg/ml aprotinin, 1 μg/ml pepstatin), pelleted (1,500 rpm, 10 min), resuspended in 0.6 ml HB-EDTA, and homogenized by 10–13 passages through a 22-gauge 1[1/4] needle. After centrifugation (2,500 rpm, 15 min) the post-nuclear supernatant (PNS) was collected, and its sucrose concentration increased under stirring to 40.6% by slow addition of 62% sucrose in HB-EDTA. PNS was then carefully overloaded with 1.5 ml of 35% and 1 ml of 25% sucrose in HB-EDTA. The tube was filled with HB, and the centrifugation was performed in an SW55Ti rotor (50,000 rpm, 66 min). The late endosome-enriched fraction was collected among 25% sucrose and HB (upper interface), the early endosome-enriched fraction (LE) among 35 and 25% sucrose (middle interface). The lower interface (40.6/35% sucrose) contained plasma membrane and other cellular compartments. Endocytic compartments were characterized by measuring enzymatic activities, by immunofluorescence, and by migration of the purified compartments in density gradients.

Self-generated Optiprep™ Density Gradient—Separation of LE and vacuoles from lysosomes and other cellular compartments was accomplished by self-generated linear gradients of Optiprep™. PNS was prepared essentially as described above, in a buffer containing 20 mM Hepes, pH 7.4, 250 mM sucrose, 1 mM EDTA, 1 μg/ml antipain, 10 μg/ml aprotinin, 1 μg/ml pepstatin. PNS was mixed with Optiprep™ to a 12.5% working solution and centrifuged to equilibrium in a NTV90 rotor (76,000 rpm, 130 min). 0.3-ml fractions were collected from the bottom of the tube with a peristaltic pump; aliquots were assayed for β-glucosaminidase and acid phosphatase activities, and the remaining material was processed for immunoblotting. In control experiments, LE derived from a flotation sucrose gradient (Fig. 1, *lane 2*) were subjected to isopycnic density centrifugation under the same conditions. SDS-PAGE analysis showed that LE collected in fractions 7–11, corresponding to the Rab7$^+$/CI-M6PR$^+$ fractions derived from isopycnic centrifugation of whole PNS.

Western Blots—After SDS-PAGE, proteins were transferred onto Immobilon-P membranes (Millipore). Membranes were saturated in 5% dry milk in TBS (20 mM Tris-HCl, pH 7.6, 133 mM NaCl) and exposed overnight to primary antibody and for 1 h to peroxidase-conjugated secondary antibody (diluted in TBS). After washings with 0.05% Tween 20 in TBS, and with TBS, proteins were detected using the enhanced chemiluminescence system and a high performance chemiluminescence film (Amersham Corp., UK). The latter was scanned with a dual-wavelength Shimadzu CS930 densitometer.

Immunofluorescence Microscopy—Twenty-four hours before experiments, BHK cells were seeded with a density of 15,000/cm^2 in 75-cm^2 Petri dishes containing glass coverslips and were then treated with 0, 5, and 50 nM VacA as described above. Coverslips were rinsed with PBS, and cells were fixed in 3% paraformaldehyde. After 2 short washings with PBS, 0.38% glycine, 0.27% NH_4Cl, and 2 additional washings with PBS, the antigen accessibility was improved by a 30-min incubation with PBS, 0.2% saponin, 0.5% bovine serum albumin. All antibodies (anti-VacA, anti-cathepsin D, anti-CI-M6PR, anti-Rab7, anti-Lgp110, and Texas Red-labeled donkey anti-rabbit) were diluted in the latter solution.

RESULTS

Characterization of Vacuoles Originated by VacA Treatment in BHK Cells by Flotation Sucrose Step Gradient—Vacuoles that form in HeLa cells exposed to VacA have components such as Rab7 and the vacuolar H^+-ATPase, characteristic of the late endosomal (LE) compartment (14, 17, 28). These vacuolar structures could arise and grow either by a homotypic LE fusion or by a heterotypic fusion of LE with lysosomal or pre-lysosomal vesicles, as recently found for wortmannin-induced vacuoles (29). In the former case, vacuoles isolated from VacA-exposed cells should have a protein profile matching that of LE isolated from control cells, whereas in the case of heterotypic fusion, the two profiles should be different.

To distinguish between these two possibilities, we compared

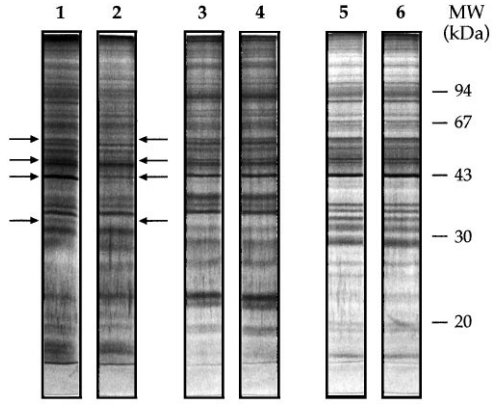

FIG. 1. **Changes of the protein pattern in LE-enriched fractions from flotation sucrose gradients.** Silver staining of an SDS-PAGE. LE-enriched fraction from BHK cells intoxicated with 5 nM VacA (*lane 1*) and from control BHK cells (*lane 2*); early endosome-enriched fraction from VacA-intoxicated (*lane 3*) and control cells (*lane 4*); lower interface of the flotation gradient from VacA-intoxicated (*lane 5*) and control cells (*lane 6*). Additional details are found under "Experimental Procedures."

by SDS-PAGE the protein profiles of endocytic compartments of BHK cells (exposed to VacA or mock-treated) isolated by sucrose step gradients. Fig. 1 shows the subtle but reproducible differences found in the electrophoretic pattern of the fractions collected from the three interfaces of the flotation gradient. Such differences (*arrows*) are restricted to the LE-enriched fractions, collected from the higher interface of the gradient and presented in *lane 1* (VacA-treated) and *lane 2* (control cells). Early endosome-enriched fractions collected from the middle (*lane 3* and *4*) and fractions collected from the lower interfaces (*lanes 5* and *6*) do not show appreciable variations. Although VacA treatment of the cells does not lead to significant changes in the distribution of Rab5, transferrin receptor, Rab7, and CI-M6PR as determined by endocytic compartments fractionation with this technique (not shown), these preliminary results represent the first evidence that the toxin produced by *H. pylori* induces changes in the protein content of the LE compartments. Changes could be ascribed to the recruitment of protein components from other compartments, resulting from heterotypic fusion events.

Redistribution of Lysosomal Type I Integral Membrane Glycoproteins Is an Early Event in VacA Intoxication—These results and the finding that VacA interferes with Rab7$^+$ endosomal compartments (16, 17, 28) prompted us to carefully investigate the distribution of a number of late endocytic and lysosomal markers in control and in VacA-intoxicated cells. For this purpose, the step gradient described in the previous section is insufficient because electron microscopy (27) and immunoblotting (not shown) reveal that at least part of the cellular population of lysosomes colocalizes with LE in the upper interface of the flotation gradient. Therefore, we optimized a self-generating, isopycnic Optiprep™ gradient, for the clear-cut separation of the late endocytic from the lysosomal compartment of BHK cells.

PNS was subjected to isopycnic ultracentrifugation and fractions were collected, denser first, and characterized by immunoblot and enzymatic activity analysis. Fig. 2 presents the position in a 12.5% Optiprep™ gradient of some of the markers tested; acid phosphatase and cathepsin B as lysosomal markers, Rab7 as LE marker, and β-glucosaminidase as a marker for both lysosomes and LE (see Ref. 23 for this choice of markers).

As expected, lysosomes, whose density is the highest among cell organelles (23), are collected from the bottom of the tube

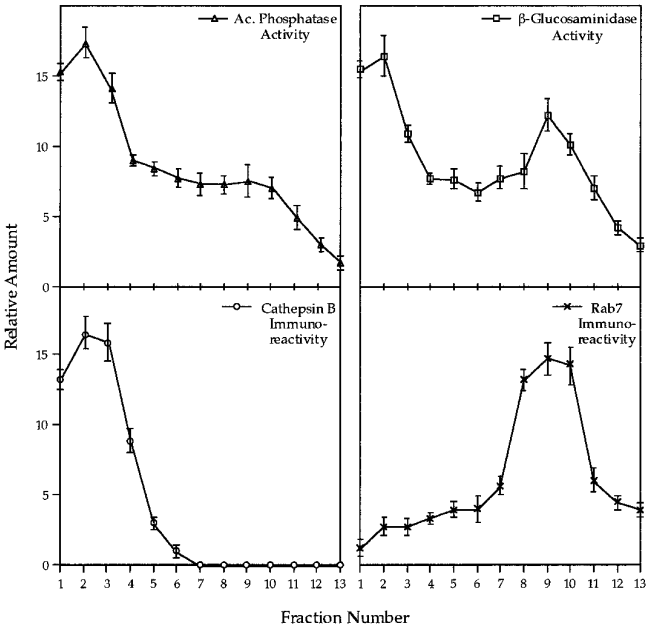

FIG. 2. **Distribution of late endosomal and lysosomal markers after isopycnic density gradient centrifugation of PNS from BHK cells.** The distribution of acid phosphatase (*Ac. phosphatase*) and β-glucosaminidase (*top panels*) has been determined by activity measurements, as reported under "Experimental Procedures." The distribution of cathepsin B and Rab7 has been determined by immunoreactivity of Optiprep™-derived fractions and quantified by scanning with a dual-wavelength Shimadzu CS930 densitometer. Experiments were performed in triplicate.

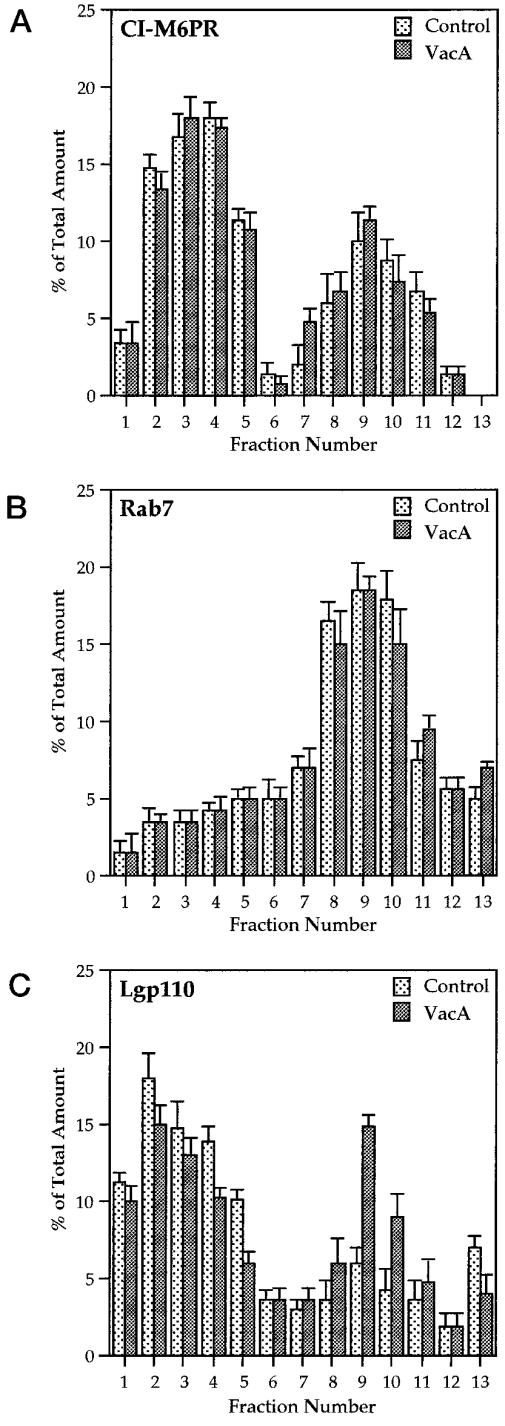

FIG. 3. **Distribution of CI-M6PR, Rab7, and Lgp110 after isopycnic density gradient centrifugation of PNS from control and from VacA-treated BHK cells.** PNS from control cells and cells incubated 4 h with 5 nM VacA were subjected to isopycnic gradient centrifugation. Fractions were subjected to gel electrophoresis, and the distribution of CI-M6PR, Rab7, and Lgp110 was determined by immunoblot and quantified by densitometry. *A*, distribution of CI-M6PR. *B*, distribution of Rab7. The distribution of these LE markers does not change significantly upon VacA treatment. *C*, distribution of Lgp110. The treatment with low nM toxin concentrations induces an important shift of Lgp110 immunoreactivity to *fractions 8–11*. *Bars* represent S.D. of two different experiments.

together with plasma membrane (alkaline phosphatase as marker, not shown) and trans-Golgi network (see below). Fig. 2 shows that the mature form of cathepsin B and the major peaks of the lysosomal enzymatic activities are detected in fractions 1–5 (lysosomes). A minor peak of β-glucosaminidase activity is also found in lighter fractions, afterward identified as LE due to the presence of late endosomal markers. In the *right panels* of Fig. 2, the peak of Rab7 immunoreactivity colocalizes (fractions 7–11) with the minor peak of β-glucosaminidase activity. These fractions are therefore enriched in LE and are clearly separated from the lysosome-containing fractions. The same analysis was then performed on cells exposed for 4 h to 5 nM VacA, but neither the lysosomal enzymatic activities nor the markers detected by immunoblot changed significantly their position in the gradient.

To compare cellular vacuoles induced by VacA with those induced by wortmannin, an inhibitor of phosphatidylinositol 3-kinase, and described in a previous study (29), we determined the position of the CI-M6PR, a trans-Golgi network and LE marker, and of Lgp110, a lysosomal membrane glycoprotein, in the fractions of the isopycnic gradient. In control cells, the CI-M6PR is immunodetected in two regions of the gradient (Fig. 3*A*) as follows: the denser one (fractions 2–5) corresponds to membranes derived from the trans-Golgi network, whereas the lighter, overlapping the distribution of Rab7 (Fig. 3*B*) and of the minor peak of β-glucosaminidase (Fig. 2), corresponds to LE compartments. The distribution of Lgp110 in the same gradient (Fig. 3*C*) is similar to the distribution of β-glucosaminidase, with a major peak corresponding to lysosomal fractions and a minor one overlapping the distribution of LE. Although there is little variation in the distribution of CI-M6PR and of Rab7 in VacA-treated cells (Fig. 3, *A* and *B*), a consistent portion of Lgp110 shifts from lysosomal fractions (*1-5* in Fig. 3*C*) to lighter fractions with a density corresponding to that of $Rab7^+$/$CI\text{-}M6PR^+$ LE of control cells (*7-11* in the same figure). This redistribution of the lysosome membrane glycoprotein Lgp110 is not accompanied by a comparable redistribution of lysosomal enzymatic activities (see below) and is evident in cells exposed to VacA at such low concentrations (5 nM) that neither macroscopic vacuoles are visible nor can an

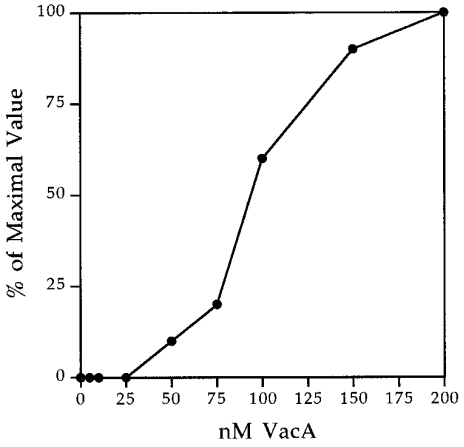

FIG. 4. **VacA activity determined by neutral red uptake.** BHK cells were treated 4 h at 37 °C with the indicated VacA concentrations in the presence of 5 mM NH_4^+. Determination of neutral red uptake was performed as described (26).

increased uptake of neutral red be measured (26) (Fig. 4). Hence, such redistribution of a lysosomal membrane protein is an early event in cellular intoxication by VacA and cannot be attributed to the gross alteration of cell structure and organization induced by filling the cytosol with large vacuoles.

Attempts to separate LE from the Lgp110-enriched compartment by changing the percentage of the Optiprep™ working solution or the modality of centrifugation were unsuccessful. Hence, it remains to be established whether VacA-intoxicated cells contain "normal" LE ($Rab7^+$/CI-$M6PR^+$) together with a distinct population of $Lgp110^+$ vacuoles with the same density, or whether VacA induces the formation and accumulation of a distinct hybrid compartment endowed with both LE and lysosomal components and having a density comparable with that of LE. The second possibility is supported by the results presented in the following section.

Characterization of the Vacuolar Structures by Immunofluorescence—Figs. 5, 6, and 7 show phase contrast (*left*) and the corresponding immunofluorescence images (*right*) of control and of VacA-treated BHK cells. Immunostaining is specific for Lgp110 (Fig. 5, *B*, *D*, and *F*), for Rab7 (Fig. 6, *B*, *D*, and *F*), and for CI-M6PR (Fig. 7, *B* and *D*). The phase contrast images of Fig. 5 show control BHK cells (*A*), cells exposed to 5 nM VacA (*C*), and to 50 nM VacA (*E*). Low nM concentration of VacA does not induce formation of vacuoles of a size detectable by phase contrast microscopy nor increases neutral red uptake (Fig. 4). However, immunofluorescence staining with a Lgp110-specific polyclonal antibody shows a labeling condensed in enlarged structures that probably represent vacuoles at an early stage of development. Moreover, as reported in the previous section, the redistribution of part of the lysosomal membrane glycoprotein from heavy to lighter fractions can already be detected by isopycnic gradient centrifugation.

In cells treated with 50 nM VacA, vacuoles are clearly visible in phase contrast (*E*) and Lgp110 is clearly localized on their membrane (*F*). These cells were also immunostained for cathepsin D, a protein of the lumen of lysosomes, but it was not found inside vacuoles (not shown). This could be ascribed to technical problems, such as its dilution in the vacuolar lumen, which is larger than that of lysosomes, or to cathepsin loss during cell fixation. However, this result parallels that obtained with isopycnic gradients, where redistribution of lysosomal membrane proteins to lighter fractions is not accompanied by an increase in hydrolytic activities.

Fig. 6 (*D* and *F*) shows that, as for Lgp110, Rab7 is clustered in enlarged structures in cells treated with 5 nM VacA and

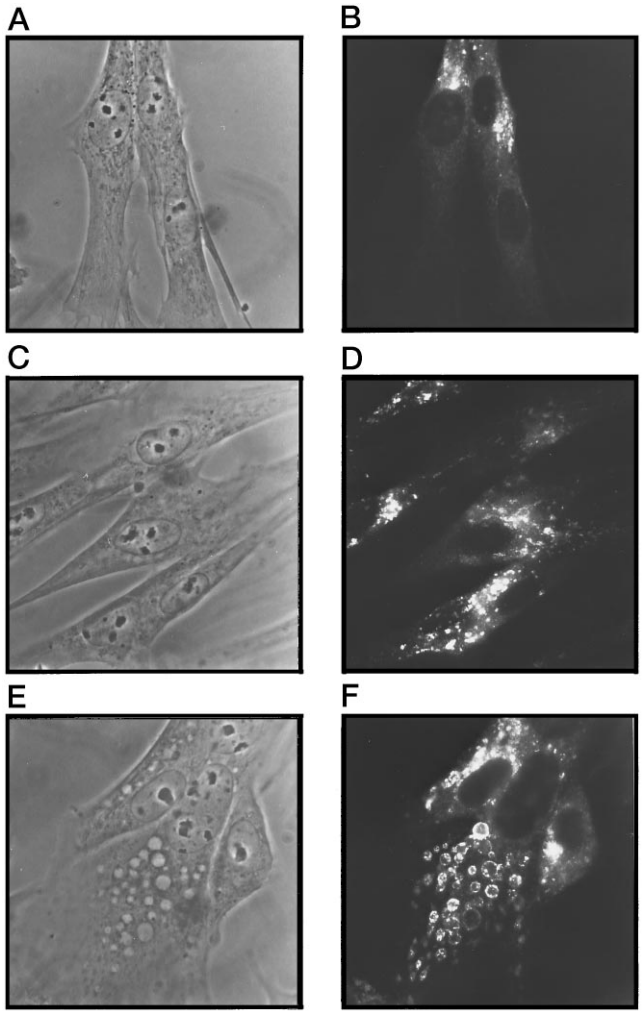

FIG. 5. **Immunofluorescence localization of Lgp110 in control BHK cells and in cells intoxicated with 5 and 50 nM VacA.** *A* and *B* represent phase contrast and immunofluorescence staining (obtained with Lgp110-specific polyclonal antibody) of control cells. *C–D* and *E–F* are the corresponding images of cells treated with 5 and 50 nM VacA, respectively.

decorates the membrane of most of the vacuoles that form upon treatment with 50 nM toxin. On the contrary, also in highly vacuolated cells, the cellular distribution of the CI-M6PR does not change (compare *B* and *D* of Fig. 7), and interestingly, vacuoles are not labeled. The presence of the lysosomal marker Lgp110, of the late endosomal marker Rab7, and the absence of another late endosomal marker (CI-M6PR) clearly indicate the post-late endosomal origin of VacA-induced vacuoles.

DISCUSSION

Cell vacuolation is the major detectable activity of VacA, which determines its name of vacuolating cytotoxin. Previous experiments aimed at the characterization of vacuoles and at the study of the mechanism of vacuolation employed toxin-enriched bacterial extracts or high concentrations of purified toxin to emphasize the phenomenon by inducing a rapid and massive cell vacuolation. *In vivo*, type I *H. pylori* strains release VacA, as clearly deduced from the presence of anti-VacA antibodies in the serum of infected people or animal models (30). Although the quantity of the toxin released *in vivo* has not yet been determined, vacuoles in number and dimension comparable with those induced in cultured cells are rarely detected in human gastric biopsies (31).

Here, cells were exposed to amounts of VacA closer to those

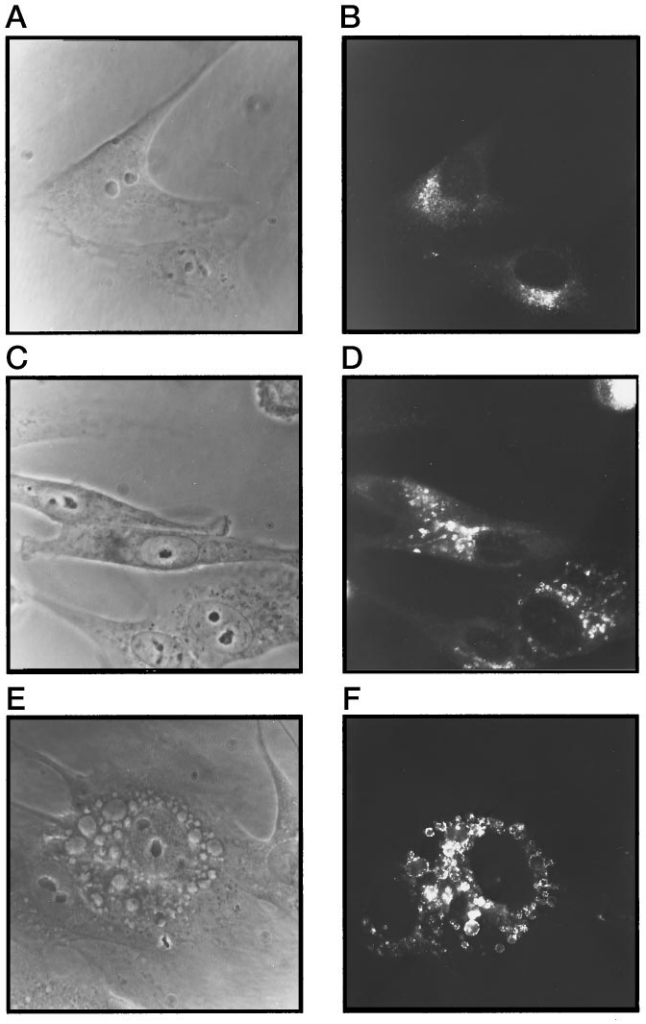

FIG. 6. **Immunofluorescence localization of Rab7 in control BHK cells and in cells intoxicated with 50 nM VacA.** *A–F* as in Fig. 6; immunofluorescence was with Rab7-specific polyclonal antibody.

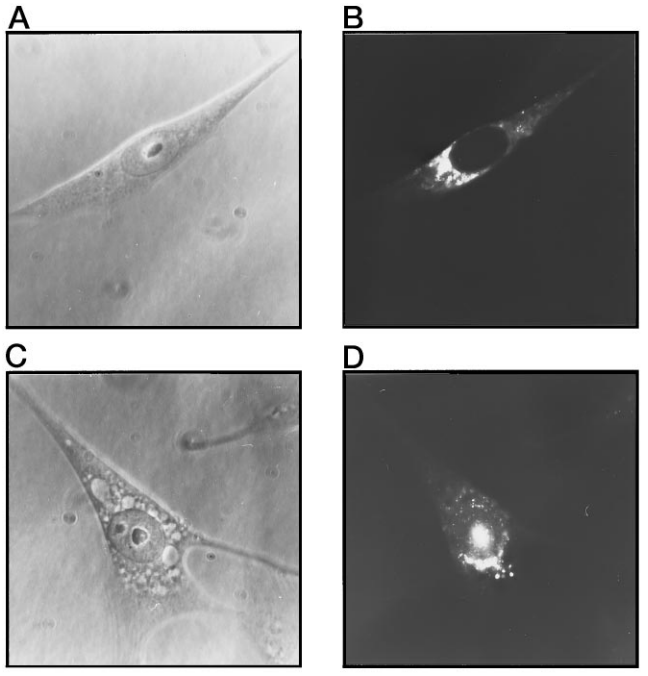

FIG. 7. **Immunofluorescence localization of CI-M6PR in control BHK cells and in cells intoxicated with 50 nM VacA.** *A* and *B* as in Figs. 5 and 6. *C* and *D* cells were treated with 50 nM VacA; immunofluorescence was with CI-M6PR-specific polyclonal antibody.

experienced *in vivo*, which are not sufficient to cause alterations detectable by phase contrast microscopy or by measuring the uptake of membrane-permeant weak bases such as neutral red. Under these conditions, VacA causes pathological changes in compartments of the endocytic pathway before vacuoles become apparent. With the aid of isopycnic density gradient centrifugation, we could follow the redistribution of Lgp110, a lysosomal membrane glycoprotein, to a compartment lighter than lysosomes, which also contains Rab7 but not CI-M6PR nor detectable amounts of cathepsin D. This novel compartment is acidic and therefore swells when osmotically active weak bases are present, thus giving rise to the large vacuoles previously associated to VacA activity. The absence of the CI-M6PR antigen and the presence of a lysosomal membrane marker identifies vacuoles as post-LE compartments. Such features are reminiscent of those of the compartment of antigen presenting cells where antigens are processed and loaded on MHC-II molecules (32). This raises the interesting possibility that VacA interferes in the antigen processing and presentation by antigen presenting cells, thus preventing T cell proliferation, an effect that would lower the immune response at the level of the stomach mucosa allowing its colonization by pathogenic strains of *H. pylori*.

Remarkably, there appears to be a non-parallel delivery of lumenal and membrane components of the lysosomes in VacA-induced vacuoles because they have a low content of hydrolytic enzymes. Such a phenomenon has already been described in the biogenesis of phagosomes in macrophages (33).

The precise sequence of events in the terminal part of the endocytic pathway, which involves LE and lysosomal compartments, is not as well characterized as that of early endocytic events (23). LE and lysosomes share several markers, but LE appear to be morphologically more complex than lysosomes, lighter and endowed with mannose-6-P receptors and Rab7 (34, 35). The presence of a heterogeneous vesicle population linking CI-M6PR$^+$/Lgp$^-$ LE to CI-M6PR$^-$/Lgp$^+$ lysosomes is known (36). A recent study postulated the existence of Rab7$^+$/CI-M6PR$^-$ intermediate vesicles, which bud from perinuclear, CI-M6PR$^+$ LE and fuse with lysosomes (22). It has also been suggested that lysosomes store mature lysosomal enzymes that are injected, when needed, in late endosomal compartments (23). Interestingly, a redistribution of lysosomal membrane glycoproteins (Lgp110 and Lgp120), similar to the one obtained by VacA, was recently described as a consequence of the treatment of NRK cells with wortmannin, an inhibitor of phosphatidylinositol 3-kinase, (29) which causes the appearance of two swollen late endocytic compartments, one Lgp$^+$/CI-M6PR$^-$ with characteristics similar to the VacA-induced vacuoles, and one positive for M6PR that was not found in VacA-treated cells. Reaves *et al.* (29) have postulated that the former compartment arises in response to the wortmannin-induced inhibition of the re-formation of electron dense lysosomes from a LE/lysosome-hybrid compartment. Similarly, it is conceivable that treatment with VacA inhibits the retrieval of membrane to lysosomes, leaving a hybrid compartment that can still fuse with more lysosomes and therefore swell, particularly in the presence of membrane-permeant amines. These analogies, first shown in the present study, suggest the possibility that phosphatidylinositol 3-kinase, is implicated in the mechanism of VacA intoxication.

Acknowledgments—We thank M. de Bernard, E. Papini, and B. Satin for stimulating discussions and Licia Bridda for collaboration in some of the experiments.

REFERENCES

1. Graham, D. Y. (1989) *Gastroenterology* **96,** 615–625
2. Goodwin, C. S. (1988) *Lancet* **ii,** 1467–1469
3. Parsonnet, J., Hansen, S., Rodriguez, L., Gelb, A. B., Warnke, R. A., Jellum, E., Orentreich, N., Vogelman, J. H., and Friedman, G. D. (1994) *N. Engl. J. Med.* **330,** 1267–1271
4. Parsonnet, J., Friedman, G. D., Vandersteen, D. P., Chang, Y., Vogelman, J. H., Orentreich, N., and Sibley, R. K. (1991) *N. Engl. J. Med.* **325,** 1127–1131
5. Isaacson, P. G. (1994) *N. Engl. J. Med.* **330,** 1310–1311
6. Tompkins, L. S., and Falkow, S. (1995) *Science* **267,** 1621–1622
7. Xiang, Z., Censini, S., Bayeli, P. F., Telford, J. L., Figura, N., Rappuoli, R., and Covacci, A. (1995) *Infect. Immun.* **63,** 94–98
8. Censini, S., Lange, C., Xiang, Z., Crabtree, J. E., Ghiara, P., Borodovsky, M., Rappuoli, R., and Covacci, A. (1996) *Proc. Natl. Acad. Sci. U. S. A.* **93,** 14648–14653
9. Telford, J. L., Dell'Orco, M., Comanducci, M., Burroni, D., Bugnoli, M., Nuti, S., Tecce, M. F., Censini, S., Covacci, A., Xiang, Z., Papini, E., Montecucco, C., Ghiara, P., Parente, L., Abrignani, S., and Rappuoli, R. (1994) *J. Exp. Med.* **179,** 1653–1658
10. Cover, T. L., Tummuru, M. K. R., Cao, P., Thompson, S. A., and Blaser, M. J. (1994) *J. Biol. Chem.* **269,** 10566–10573
11. Schmitt, W., and Haas, R. (1994) *Mol. Microbiol.* **12,** 307
12. Moll, G., Papini, E., Colonna, R., Burroni, D., Telford, J., Rappuoli, R., and Montecucco, C. (1995) *Eur. J. Biochem.* **234,** 947–952
13. Montecucco, C., Papini, E., and Schiavo, G. (1994) *FEBS Lett.* **346,** 92–98
14. Papini, E., Bugnoli, M., de Bernard, M., Figura, N., Rappuoli, R., and Montecucco, C. (1993) *Mol. Microbiol.* **7,** 323–327
15. Leunk, R. D. (1991) *Rev. Infect. Dis.* **13,** 686–689
16. Papini, E., de Bernard, M., Milia, E., Bugnoli, M., Zerial, M., Rappuoli, R., and Montecucco, C. (1994) *Proc. Natl. Acad. Sci. U. S. A.* **91,** 9720–9724
17. Papini, E., de Bernard, M., Satin, B., Gottardi, E., Telford, J., Manetti, R., Zerial, M., Rappuoli, R., and Montecucco, C. (1996) in *Bacterial Protein Toxins* (Frandsen, F., ed) Vol. 28, pp. 181–189, Gustav Fischer Verlag, Stuttgart/Jena/New York
18. Aniento, F., Emans, N., Griffiths, G., and Gruenberg, J. (1993) *J. Cell Biol.* **123,** 1373–1387
19. Bucci, C., Parton, R. G., Mather, I. H., Stunnenberg, H., Simons, K., Hoflack, B., and Zerial, M. (1992) *Cell* **70,** 715–728
20. Clague, M. J., Urbé, S., Aniento, F., and Gruenberg, J. (1994) *J. Biol. Chem.* **269,** 21–24
21. Feng, Y., Press, B., and Wandinger-Ness, A. (1995) *J. Cell Biol.* **131,** 1435–1452
22. Méresse, S., Gorvel, J.-P., and Chavrier, P. (1995) *J. Cell Sci.* **108,** 3349–3358
23. Griffiths, G. (1996) *Protoplasma* **195,** 37–58
24. Manetti, R., Massari, P., Burroni, D., DeBernard, M., Marchini, A., Olivieri, R., Papini, E., Montecucco, C., Rappuoli, R., and Telford, J. L. (1995) *Infect. Immun.* **63,** 4476–4480
25. de Bernard, M., Papini, E., de Filippis, V., Gottardi, E., Telford, J., Manetti, R., Fontana, A., Rappuoli, R., and Montecucco, C. (1995) *J. Biol. Chem.* **270,** 23937–23940
26. Cover, T. L., Puryear, W., Perez-Perez, G. I., and Blaser, M. J. (1991) *Infect. Immun.* **59,** 1264–1270
27. Gorvel, J.-P., Chavrier, P., Zerial, M., and Gruenberg, J. (1991) *Cell* **64,** 915–925
28. Papini, E., Satin, B., Bucci, C., de Bernard, M., Telford, J., Manetti, R., Rappuoli, R., Zerial, M., and Montecucco, C. (1997) *EMBO J.* **16,** 15–24
29. Reaves, B. J., Bright, N. A., Mullock, B. M., and Luzio, J. P. (1996) *J. Cell Sci.* **109,** 749–762
30. Marchetti, M., Aricò, B., Burroni, D., Figura, N., Rappuoli, R., and Ghiara, P. (1995) *Science* **267,** 1655–1658
31. Fiocca, R., Villani, L., Luinetti, O., Gianatti, A., Perego, M., Alvisi, C., Turpini, F., and Solcia, E. (1992) *Virchows Arch. A Pathol. Anat.* **420,** 489–498
32. Fernandez-Borja, M., Verwoerd, D., Sanderson, F., Aerts, H., Trowsdale, J., Tulp, A., and Neefjes, J. (1995) *Infect. Immun.* **8,** 625–640
33. Desjardins, M. (1995) *Trends Cell Biol.* **5,** 183–186
34. Ludwig, T., Le Borgne, R., and Hoflack, B. (1995) *Trends Cell Biol.* **5,** 202–206
35. Zerial, M., and Stenmark, H. (1993) *Curr. Opin. Cell Biol.* **5,** 613–620
36. Geuze, H. J., Stoorvogel, W., Strous, G. J., Slot, J. W., Bleekemolen, J. E., and Mellman, I. (1988) *J. Cell Biol.* **107,** 2491–2501

Vacuoles Induced by *Helicobacter pylori* Toxin Contain Both Late Endosomal and Lysosomal Markers

Maurizio Molinari, Carmela Galli, Nathalie Norais, John L. Telford, Rino Rappuoli, J. Paul Luzio and Cesare Montecucco

J. Biol. Chem. 1997, 272:25339-25344.
doi: 10.1074/jbc.272.40.25339